HHS Public Access

Author manuscript

J Nanomed Nanotechnol. Author manuscript; available in PMC 2016 November 01.

Published in final edited form as:

J Nanomed Nanotechnol. 2015 November ; 6(Suppl 6): . doi:10.4172/2157-7439.S6-006.

Cardiac Ischemia Reperfusion Injury Following Instillation of 20 nm Citrate-capped Nanosilver

NA Holland[1], **DP Becak**[1], **Jonathan H Shannahan**[2], **JM Brown**[2], **SA Carratt**[3], **LSV Winkle**[3], **KE Pinkerton**[3], **CM Wang**[4], **P Munusamy**[4], **Don R Baer**[4], **SJ Sumner**[5], **TR Fennell**[5], **RM Lust**[1], and **CJ Wingard**[1,*]

[1]Department of Physiology, Brody School of Medicine at East Carolina University, Greenville, North Carolina, USA

[2]Department of Pharmaceutical Sciences, Skaggs School of Pharmacy and Pharmaceutical Sciences, The University of Colorado Anschutz Medical Campus, Aurora, USA

[3]Department of Anatomy, Physiology and Cell Biology, School of Veterinary Medicine, University of California at Davis, Davis, California, USA

[4]Pacific Northwest National Laboratory, EMSL, Richland, USA

[5]RTI International, Discovery Sciences, Research Triangle Park, USA

Abstract

Background—Silver nanoparticles (AgNP) have garnered much interest due to their antimicrobial properties, becoming one of the most utilized nano-scale materials. However, any potential evocable cardiovascular injury associated with exposure has not been reported to date. We have previously demonstrated expansion of myocardial infarction after intratracheal (IT) instillation of carbon-based nanomaterials. We hypothesized pulmonary exposure to Ag core AgNP induces a measureable increase in circulating cytokines, expansion of cardiac ischemia-reperfusion (I/R) injury and is associated with depressed coronary constrictor and relaxation responses. Secondarily, we addressed the potential contribution of silver ion release on AgNP toxicity.

Methods—Male Sprague-Dawley rats were exposed to 200 μl of 1 mg/ml of 20 nm citrate-capped Ag core AgNP, 0.01, 0.1, 1 mg/ml Silver Acetate (AgAc), or a citrate vehicle by intratracheal (IT) instillation. One and 7 days following IT instillation the lungs were evaluated for

[*]**Corresponding author:** Wingard CJ, Department of Physiology, Brody School of Medicine at East Carolina University, Greenville, North Carolina, USA, Tel: 252-744-2804; wingardc@ecu.edu.

Competing Interests

The authors declare that they have no competing interests.

Authors' Contributions

NAH performed the I/R and cytokine experimental design data analysis and interpretation and drafted the manuscript. DPB performed the coronary vessel wire myography and BALF data analysis and interpretation. JHS and JMB performed the darkfield microscopy, data analysis, and interpretation. SAC, LSVW, and KEP performed the autometallography experiments, data analysis and interpretation. CMW, PM, and DRB performed the AgNP characterization experiments as well as data analysis and interpretation. SJS, TRF, RML, and CJW participated in the study design, data interpretation and editing of the manuscript. CJW was responsible for the study design and the coordination of experiments. All authors read and approved of the final manuscript.

inflammation and the presence of silver; serum was analyzed for concentrations of selected cytokines; cardiac I/R injury and coronary artery reactivity were assessed.

Results—AgNP instillation resulted in modest pulmonary inflammation with detection of silver in lung tissue and alveolar macrophages, elevation of serum cytokines: G-CSF, MIP-1α, IL-1β, IL-2, IL-6, IL-13, IL-10, IL-18, IL-17α, TNFα, and RANTES, expansion of I/R injury and depression of the coronary vessel reactivity at 1 day post IT compared to vehicle treated rats. Silver within lung tissue was persistent at 7 days post IT instillation and was associated with an elevation in cytokines: IL-2, IL-13, and TNFα and expansion of I/R injury. AgAc resulted in a concentration dependent infarct expansion and depressed vascular reactivity without marked pulmonary inflammation or serum cytokine response.

Conclusions—Based on these data, IT instillation of AgNP increases circulating levels of several key cytokines, which may contribute to persistent expansion of I/R injury possibly through an impaired vascular responsiveness.

Keywords

Pulmonary exposure; Myocardial infarction; Coronary artery; Serum cytokines; Nanotoxicology

Introduction

In recent decades, advances in material sciences and engineering have yielded new classes of nano-sized materials. These nanomaterials have a size range of between 1 nm and 100 nm in at least one dimension and are characterized by a high surface to mass ratio [1,2]. Of the various forms of engineered nano materials (ENM), silver nanoparticles (AgNP) have garnered much attention for potential uses in commercial applications. Silver exhibits innate antimicrobial properties [3] which have made AgNP attractive for biomedical and consumer applications including but not limited to: wound dressings, silver impregnated catheters, vascular prosthetics, clothing and undergarments, air filters, laundry detergents, toiletries, and water taps [2,4].

However, despite the seemingly ubiquitous use of AgNP, the toxicity of these ENM, particularly the cardiovascular toxicity, is poorly understood. Furthermore, mechanisms by which AgNP may interact with biological interfaces are only beginning to be elucidated [5,6]. Silver ions bind to both sulfur and phosphate molecules [2], which may interrupt normal cellular membrane function as well as disrupt DNA and RNA binding [7]. In metal derived nanomaterials [8] and the interactions of ENM *in vivo*, nanoparticle size and chemical composition may be an important factor in determining toxicological impact of AgNP exposure. Surface oxidation of AgNP may lead to oxidative stress and interactions with macromolecules that alter signaling processes, contributing to cardiovascular dysfunction following pulmonary exposure to AgNP [9,10].

Inhalation exposure to aerosolized particles is a chief concern regarding the safety of engineered nanomaterials. Aerosolization of particles may ᵒᶜcur at several phases of AgNP manufacture and utilization. Inhalation exposure to AgNP is most likely to occur during particle synthesis, handling of dry powders, aerosolization of liquid suspensions, as well as

the manufacture and machining of composites containing AgNP [11]. Exposure is also possible outside of the realm of occupational exposure, through the use of AgNP in consumer products such as disinfecting sprays or deodorants that have the potential to directly aerosolize AgNP, which could lead to a direct pulmonary exposure to AgNP [11].

In order to address potential concerns regarding the human health effects of exposure to nanomaterials the National Institute of Environmental Health Sciences Centers for Nanotechnology Health Implications Research (NCNHIR) Consortium was organized to gain a comprehensive and systematic understanding of ENM's biological interactions as influence by their physiochemical properties. The underlying mechanisms by which ENM may impact the cardiovascular system are unclear. Proposed mechanisms of ENM cardiovascular toxicity may include systemic inflammation, metabolic derangement, autonomic dysregulation or oxidative stress [12,13]. Previous investigations have demonstrated that exposure to various other particulate and ENM was associated with an increased inflammatory response as well as cardiovascular dysfunction [14–17]. Here we investigated the cardiovascular impact of an acute pulmonary exposure to a silver salt and pure silver core nanoparticle formulated with citrate-capping (AgNP) at 1 day and 7 days following exposure. We hypothesized that pulmonary exposure to AgNP results in a pro-inflammatory state originating in the lungs that drives the expansion of cardiac ischemia-reperfusion (I/R) injury associated with increased serum cytokines not seen with the silver salt. To test this hypothesis male Sprague-Dawley (SD) rats were examined following intratracheal (IT) instillation of 200 μg of AgNP at 1 or 7 days following instillation. Lungs and BAL cells were collected for assessment of injury, inflammation and silver persistence. In addition, serum was collected and measured for selected circulating cytokines. Rats underwent a temporary occlusion of the left anterior coronary artery to determine the impact of AgNP on expansion of myocardial infarction. To further elucidate the cardiovascular impact of pulmonary exposure to AgNP, *ex vivo* small vessel wire myography was utilized to assess the reactivity of the left anterior descending coronary artery. Additionally, to test the contribution of ionic silver released from AgNP on the cardiovascular toxicology associated with AgNP exposure, cohorts of animals were instilled with silver acetate (2 μg–200 μg silver as AgAc) and cardiovascular injury endpoints and circulating cytokine profile were evaluated.

Materials and Methods

Animals

Male Sprague Dawley rats 51–54 days of age and weighing 201–225 grams were purchased from Charles River Laboratory (Raleigh, NC, USA). Rats were housed two per cage under a 12 hour light/dark cycle. Standard rat chow and water were provided ad libidum. All animals were allowed a 1 week acclimatization period before beginning experimentation. Animals were randomly assigned to the following experimental groups for 1 day and 7 days post-instillation analysis: Naïve, Citrate, 20 nm AgNP/Citrate. Additional experimental groups included a 24 hour exposure to: 0.01, 0.1, and 1 mg/ml AgAc. ECU Institutional Animal Care and Use Committee approved all animal handling and experimental procedures.

Nanomaterials, AGAC, vehicles, and characterization

Twenty nm AgNP were procured from NanoComposix (San Diego, CA) though the NIEHS Centers for Nanotechnology Health Implications Research (NCNHIR) Consortium. Particle characterization as reported by the manufacturer included: A) Diameter (TEM) 21.3 ± 3.2 nm; B.) Surface Area (TEM) 25.6 m^2/g; C.) Hydrodynamic Diameter (DLS) 26.2 nm; D.) Zeta Potential −34.4 mV; and endotoxin concentration<5 EU/ml. The vehicle control for citrate AgNP was a 2 mM solution of sodium citrate dissolved in deionized water. The citrate capped silver nanoparticles stocks were independently characterized by Pacific Northwest National Laboratory's Environmental Molecular Sciences Laboratory. Effective particle size (29.5 ± 0.5 nm) Polydispersity Index (0.180) and Zeta Potential (−38 ± 1 mV) were assessed using a Brookhaven ZetaPALS Instrument (Brookhaven Instruments Corporation, Holtsville, NY). Scanning Transmission Electron Microscopy (S/TEM) was also performed (Supplemental Figure 1). Stock samples were provided at concentration 1 mg/ml, stock particle suspension was stored in the dark at 2–8°C. Silver Acetate was provided by RTI International (Research Triangle Park, NC) as purchased from Sigma-Aldrich (St. Louis, MO, USA). Silver Acetate was dissolved in sterile H_2O at a concentration of 1.62 mg /ml to create an ionic silver concentration of 1.0 mg/ml. Dilutions were made from an aliquot of the 1.0 mg/ml AgAc to yield 0.1mg/ml AgAc and 0.01mg/ml AgAc. All sliver solutions and dry AgAc were stored at 4°C and kept from light.

Instillate preparation, dosing, and intratracheal instillation

AgNP aliquots were cup-horn sonicated (Misonix Model 1510r-MTH, Branson Ultrasonics Corp. Danbury, CT) for 30 seconds at 50% amplitude. Sonicated aliquots were then vortexed for 30 seconds prior to instillation. Rats were anesthetized by inhalation of a 50:50 isoflurane propylene-glycol mixture in an induction chamber. Once an adequate plane of anesthesia had been achieved the rat was vertically suspended by the frontal incisors. The tongue of the rat was anteriorly displaced and 200 ul of AgNP, AgAc or vehicle was dispensed into the glottal opening during inspiration to ensure pulmonary aspiration.

Cardiac ischemia/reperfusion and quantification of infarct size

One or 7 days following IT instillation rats were anesthetized with an intramuscular injection of ketamine/xylazine (90/10 mg/kg, respectively). Body temperature was maintained at 37°C with a heating pad and feedback control using a rectal temperature probe and TC-1000 Temperature Controller (CWE, Inc., Ardmore, PA). Once anesthetized the rats were intubated via tracheostomy with a 16 gauge angiocatheter. Rats were ventilated with fraction of inspired oxygen (FiO_2) of 1 via an Inspira Advanced Safety Ventilator (Harvard Apparatus, Holliston, MA) with a 3 ml tidal volume at 81 breaths per minute. Each animal was allowed at least 15 minutes of equilibration prior to any baseline data collection prior to ischemic manipulation.

The heart was exposed by an anterolateral partial sternotomy. The LAD was visualized and occluded with 6-0 prolene suture and PE 90 with a flared end as a reversible tourniquet. The tourniquet was secured in place for a 20 minute period of ischemia. Successful occlusion of the LAD was confirmed by: A.) blanching of the myocardium distal to the occlusion, B.)

myocardial dyskinesia, and C.) ECG changes. Following 20 minutes of ischemia the reversible tourniquet was released allowing two hours of reperfusion.

Following the reperfusion period the rat was exsanguinated by transection of the inferior vena cava. The descending thoracic aorta was then cannulated with PE 90 and advanced to the coronary ostia. The heart was flushed with approximately 5 ml 0.09% normal saline and the LAD was re-occluded and infused with 1% Evans blue dye for demarcation of the non at risk myocardium. The heart was then excised and sliced into approximate 1mm sections distal to the occlusion. The slices were incubated in 0.25% TTC (Sigma-Aldrich, St. Louis, MO) for 10 minutes to determine viable from infarcted tissue. Both sides of each heart slices were digitally photographed and Image J (National Institutes of Health) was used to quantify the area of the left ventricle, area at risk, and area of infarction.

Coronary artery isolation and pharmacology

Coronary artery isolation and vessel viability assessment were performed 1 or 7 days following IT exposure to AgNP or 1 day following IT exposure to citrate vehicle or AgAc. Isolation of the coronary artery was performed as previously described [18]. The heart was excised and placed in ice-cold physiological saline solution (PSS); [mM] 140.0 NaCl, 5.0 KCl, 1.6 $CaCl_2$, 1.2 $MgSO_4$, 1.2 3-[N-morpholino]-propane sulfonic acid, 5.6 D-glucose, and 0.02 EDTA (pH 7.4 @ 37°C). Pairs of ~2 mm segments of left anterior descending coronary artery (LAD) were excised and mounted into the chambers of a 610M multichannel myograph (DMT, Ann Arbor, MI). Vessel lumen diameter was adjusted so that resting tension was 90% of the wall tension at 13.3 kPa. Tissue viability was assessed with a potassium depolarization using 109 mM K^+PSS (Na^+ substituted with K^+ in an equal molar fashion). Segments were washed with fresh PSS and endothelial integrity was assessed using a 1.0 μM serotonin (5-HT) stimulation followed 3.0 μM acetylcholine (ACh). A relaxation response of >50% loss of the serotonin stress was considered acceptable endothelial integrity. Segments were washed every 10 minutes with fresh PSS for 30 minutes and subject to pharmacologic assessments [19]. Paired LAD segments were subjected to cumulative concentrations of serotonin (10 nM–3.0 μM). The coronary artery stress (mN/mm^2) generated in response to 5-HT of paired segments was averaged at each concentration for data reporting. Upon establishing stable tension after addition of the highest concentration of 5-HT, one of the paired segments was subject to endothelial-dependent relaxation with ACh (1.0 nM–1.0 μM) and the other segment was subjected to endothelial-independent relaxation with sodium nitroprusside (SNP, 1.0 nM–1.0 μM).

Serum collection

Following anesthesia cardiac puncture of the right ventricle was performed to collect whole blood. Approximately 1ml of whole blood was collected from citrate, AgNP and AgAc exposed groups at 1 and/or 7 day time points. All samples were held at room temperature for approximately 30 minutes before being centrifuged at 20,800 rcf for 30 minutes at 4°C. Serum supernatant was removed from the sample, snap frozen in liquid N_2 and stored at −80°C.

Quantification of serum cytokines

Concentrations of serum: G-CSF, GM-CSF, MIP-1α, IL -1β, IL-2, IL-5, IL-6, IL-10, IL-13, IL-17α, IL-18, IFNγ, RANTES, and TNFα were measured at 1 or 7 days post-instillation using Milliplex MAP Cytokine/Chemokine Panels (EMD Millipore, Billerica, MA) according to the manufacturer's instructions. The multiplex cytokine assays were run on a MagPix system (Luminex, Austin, TX) and all results were reported and analyzed by Milliplex Analyst version 5.1 (EMD Millipore, Billerica, MA).

Bronchoalveolar lavage and cell differential

Sprague Dawley rats were euthanized and bronchoalveolar lavage was performed with a modified procedure as described by Katwa et al. [14]. Rats were deeply anesthetized with isoflurane and euthanized by pneumothorax. The thoracic cage was removed and the connective tissue surrounding the lung was resected. The left main bronchus was ligated. A tracheotomy was performed with a 14 gauge angiocatheter and secured with 2–0 suture. A bolus of Hanks balanced saline solution (23.1 ml/kg) was slowly lavaged into the right lung three successive times. Recovered BAL fluid was centrifuged at 1,000×g for 10 min at 4°C. The cell pellets were re-suspended in 1 ml of fresh cold Hanks balanced saline solution. Total cell counts were determined with a Cellometer Auto X4 (Nexcelom Biosciences, LLC, Lawrence, MA). BAL fluid volumes containing 20,000 cells were centrifuged onto glass slides using a Cytospin III (Shandon Scientific Ltd, Cheshire, UK) and stained via a three-step hematology stain (Richard Allan Scientific, Kalamazoo, MI). Cell differential counts were determined by microscopy based on hematologic stain and cellular morphology counting 300 cells per slide.

Total protein quantification of bronchoalveolar lavage fluid

Recovered BAL supernatant was used for protein quantification using a standard Bradford protein assay. Protein concentration was quantified using 5 μl of BAL supernatant diluted in 250 μl of Bradford reagent. Samples were plated in duplicate using a 96-well plate. Absorbance values were read at 562 nm using a BIO-TEK Synergy HT plate reader (Winooski, VT) and data were analyzed with Gen5 software (BIO-TEK). Absorbance values for each sample were compared with a standard curve produced using 2.0–0.0625 mg/ml of bovine serum albumin.

Lung histology

The unlavaged left lungs of instilled rats were perfused with unbuffered zinc formalin (Richard Allan Scientific) at 30 cm H_2O via an 18 gauge angiocatheter inserted into the tracheal opening. The cannulated trachea and left lung were excised intact and submerged in zinc formalin and allowed to fix for 24–72 hours before being processed and embedded in paraffin. Longitudinal lung sections (5 μm) were cut and mounted on glass slides and stained with hematoxylin and eosin (H&E) for gross pathologic and morphologic analysis using light microscopy.

Darkfield microscopy

Silver nanoparticle deposition was qualitatively evaluated in H&E stained paraffin embedded lung sections and broncholveolar lavage (BAL) cells using a Cytoviva enhanced dark field microscope (Cytoviva, Auburn, AL). Lung sections and BAL cells were evaluated, at a magnification of 60X by imaging of the cells in the focal plane of the nuclei, for presence of AgNP and qualitative assessment of AgNP deposition at 1 and 7 days following exposure.

Autometallography

Silver was visualized using a variation of a published method for autometallography [20,21]. A silver enhancement kit for light and electron microscopy (Ted Pella Inc, Redding CA) was used [6] and all slides were developed under identical conditions to facilitate comparisons across groups and time-points. Paraffin embedded samples were de-paraffinized rehydrated and stained with equal volumes of enhancer and developer for 15 minutes. Slides were imaged using an Olympus BH-2 light microscope.

Statistical analysis

All data are presented as mean values ± SEM unless otherwise noted. GraphPad Prism software version 6 (LaJolla, CA) was used for the purposes of statistical analysis and graphing with a P-value of <0.05 indicated statistical significance unless otherwise noted. Cardiac I/R, BALF cell differentials, and BALF protein quantification data were compared by one-way ANOVA with Tukey's post-hoc test for multiple comparisons. Time point differences between vehicle and AgNP exposure was conducted with a Student's t-test. Cytokines were compared by One-way ANOVA with Tukey's post-hoc test for multiple comparisons. Group size was calculated based on power analysis of cardiac I/R experiments. Coronary artery vascular response curves were generated using nonlinear regression analysis of the f-pair parameter best-fit values. Curves were compared using ANOVA with Tukey's post-test for multiple comparisons. EC_{50} and Hillslope values were generated by averaging normalized concentration-response curves (0–100%) of individual subjects within a cohort. Results were compared using ANOVA and Tukey's post-test for multiple comparisons.

Results

Pulmonary responses to instillation of AgNp or AgAc

One and 7 days following IT instillation of citrate vehicle or 20 nm AgNP, examination of hematoxylin and eosin stained lung sections of male SD rats revealed minimal acute injury associated with 20 nm AgNP. One day post instillation (Figure 1D) AgNP-instilled lungs displayed a lack of inflammation, cellular infiltrate, and alveolar wall thickening when compared to the lungs of naïve (Figure 1A) or citrate vehicle controls (Figure 1B). However, seven days following IT instillation of 20 nm AgNP a modest alveolar wall thickening was noted (Figure 1E) compared to naïve (Figure 1A) or citrate vehicle control lungs (Figure 1C). No other signs of cellular infiltrate or inflammation were noted in the lungs at 7 days following instillation.

Cell differentials within recovered bronchoalveolar fluid (BALF) demonstrated increased numbers of epithelial cells in the citrate vehicle instilled group compared to naïve. The numbers of macrophages, neutrophils, lymphocytes, or eosinophils did not differ between the naïve, citrate or 20 nm AgNP instilled groups. However, the AgAc group had lower macrophage with increased neutrophil and lymphocyte numbers than all other groups (Table 1). Protein concentration in recovered BALF also did not differ significantly between naïve, citrate control, or 20 nm AgNP groups 1 day and 7 days following instillation while the AgAc group had a greater amount of lavage protein (Table 2).

Autometalography staining of lung tissue revealed an absence of silver in alveolar spaces in naïve samples and samples from rats exposed to citrate vehicle at 1 and 7 days (Figures 2A–2C). Intratracheal instillation of AgNP resulted in positive silver staining localized to small blood vessels, type I alveolar cells in bronchiole-alveolar duct regions and macrophages in proximal airways 1 day post exposure (Figure 2D). Seven days post exposure, silver staining was present in terminal bronchial epithelial tissue, surrounding alveolar tissue as well as macrophages (Figure 2E).

Enhanced dark field microscopy also revealed the presence of silver nanoparticles in the alveoli of 20 nm AgNP instilled SD rats. The observed nanoparticles appear to be localized to alveolar macrophages rather than to epithelial cells of the alveoli at 1 day (Figure 3D) compared to vehicle (Figure 3B) or naïve (Figure 3A). Seven days following instillation, the AgNP still appeared localized to macrophages within the alveoli (Figure 3E), no AgNP were noted in citrate control lungs (Figure 3C). Examination of cells recovered from BALF with enhanced dark field microscopy shows AgNP in macrophages at 1 day and 7 days (Figures 4C and 4D) but not in macrophages recovered from citrate-instilled rats (Figures 4A and 4B).

Serum cytokine concentations following it instillation of AgNp

Analysis by multi-plex assay of serum collected from rats exposed to citrate vehicle or 20 nm AgNP revealed an increase in several cytokines and chemokines at both 1 and 7 days post instillation compared to citrate vehicle. Notably, serum concentrations of pro-inflammatory cytokines: IL-1β (Figure 5A), IL-6 (Figure 5C), IL-18 (Figure 5E), TNFα (Figure 5G), were significantly elevated at 1 day compared to citrate control. Several other cytokines and chemokines were also elevated compared to control including: G-CSF, MIP-1α, IL-2, IL-13, IL-10, IL-17α, and RANTES (Table 3). Seven days following IT instillation of 20 nm AgNP or citrate vehicle resulted in a significant elevation of cytokines: IL-2, IL-13 (Table 3) and TNFα (Figure 5H). AgAc instillation did not result in any significant release of circulating cytokines 1 day post exposure (Table 3). Serum levels of: IL-1β (Figure 5A), IL-6 (Figure 5C), IL-18 (Figure 5E), TNFα (Figure 5G) were not detectable in serum or significantly lower when compared to citrate vehicle and AgNP results (Figure 5).

Cardiovascular responses to it instillation of AgNp or AgAc

Exposure to AgNP altered coronary artery responses at 1 day and 7 days post IT instillation and in general any changes associated with exposure waned between 1 and 7 days. One day

following instillation coronary arteries isolated from AgNP instilled SD rats did not have differences in the serotonin (5-HT) maximal stress generation or EC_{50} value when compared to naïve (Figure 6A and Table 4). Instillation of the citrate vehicle depressed coronary artery stress generation capacity in response to 5-HT when compared to naïve (Figure 6A). In contrast, at seven days following exposure to AgNP there was a decrease in 5-HT stimulated response compared to naïve, manifested as a reductions in EC_{50} and Hill slope values (Table 4 and Figure 6A).

Instillation of AgNP as well as citrate vehicle decreased the magnitude of the relaxation response to acetylcholine (ACh) both 1 and 7 days following exposure (Figure 6C). However, 7 days post-exposure to AgNP increased the sensitivity (diminished EC_{50} value) to ACh compared to either naïve or 1 day post AgNP exposure (Figure 6D and Table 4). The magnitude of relaxation responses to sodium nitroprusside (SNP) was unaltered across all groups or time points (Figure 6E). However, both citrate vehicle and 7 day post-AgNP exposure displayed increased sensitivity (diminished EC_{50} value) to SNP compared to 1 day post exposure AgNP or naïve control (Figure 6 and Table 4).

Exposure to intratracheal instillation of 1 mg/ml (200 μg) AgAc did show a modest diminution but non statistical changes in magnitude of stress response, EC_{50} or Hillslope values with 5-HTstimulation when compared to naïve at 1 day following exposure (Table 4 and Supplemental Figures 2A and 2B). Intratracheal instillation of AgAc also resulted in a modest but non statistical reduction in the ACh relaxation without differences in the EC_{50} or Hillslope values (Table 4 and Supplemental Figures 2C and 2D). Exposure to AgAc did not change the relaxation characteristics, EC_{50}, or Hill slope induced by SNP concentration-response (Table 4 and Supplemental Figures 2E and 2F). Overall, instillation of AgAc stress generation and stress relaxation responses were similar to those observed for the citrate vehicle control.

Induction of cardiac I/R injury 1 day following instillation of 20 nm AgNP resulted in an increase in infarcted myocardium. The area of infarcted myocardium when normalized to the area at risk and was increased by 12% compared to naïve control (Figure 7A) and by 9% compared to the infarcted myocardium of the vehicle control (Figure 7A). The area of myocardium infarcted, within an area of risk, did not differ significantly between naïve and citrate controls at 1 day post instillation (Figure 7A). The single instillation of AgNP resulted in an expansion of cardiac I/R injury 7 days post instillation (Figure 7B). Although the size of the I/R injury following AgNP instillation appeared to be waning between the 1 and 7 day time points, they were not statistically different from each other. The naïve and citrate controls did not differ significantly in the area of myocardial infarction between the same time points.

Exposure to AgAc instillation also resulted in expansion of I/R injury in a concentration-dependent manner. Intratracheal exposure to 1 mg/ml of AgAc (200 μg) as well as 0.1 mg/ml (20 μg) resulted in an expansion of I/R injury by 21 and 11% respectively, compared to naïve (Figure 7C). The lowest concentration of AgAc instilled, (0.01 mg/ml or 2 μg), did not result in expansion of cardiac I/R injury compared to naïve (Figure 7C).

Discussion

This study is unique as it demonstrates that IT exposure to 20 nm AgNP results in exaggerated cardiovascular injury 1 and 7 days following a single bolus instillation. These findings are congruent with other studies that have investigated the potential for a negative cardiovascular impact following pulmonary exposures to various nanomaterials [15,18,22]. One hypothesis proposes that the pulmonary instillation of a nanomaterial establishes a pro-inflammatory condition that primes the target organ for exacerbation of an evoked injury response such as cardiac I/R. We provide evidence in support of such a hypothesis. With this model of IT instillation of AgNP increased serum concentrations of several cytokines and chemokines, associated with the expansion of cardiac I/R injury and an altered agonist sensitivity or [23] constrictor response of the coronary artery. We also demonstrated a cardiac ischemic reperfusion injury response to a pulmonary instillation of ionic silver in the form of AgAc but contrasts the results of the AgNp data as there was no apparent association with systemic cytokine elevation or corresponding vascular tissue response changes suggestive of an alternative mechanism of toxicity with silver ions instillation.

The link between cardiovascular disease or dysfunction and inflammation are well documented [24–26]. In this study we observed an elevation in serum concentrations, at 1 day post AgNP instillation, of pro-inflammatory cytokines: IL-1β, IL-6, IL-18, TNFα, in concentrations higher than in serum from the citrate vehicle control rats. These cytokines are well documented to have key roles in the exacerbation of cardiac injury [24,27] and increased serum concentrations have been correlated with worsening cardiac function and heart failure [24,28]. IL-1β and TNFα, in addition to IL-18 are responsible for enhanced surface expression of selectins, VCAM-1 and ICAM-1 [29,30], which indicate endothelial activation due to inflammation. Inflammatory induction of the endothelium may play a role in influencing those vascular response as changes seen in this study and reported to be associated with particle exposure and no-reflow phenomenon [25,29] underlying an expansion of cardiac I/R injury. The profile of elevated cytokines may contribute to the observed coronary vascular dysfunction. Elevations in cytokines such as IL-2 and TNFα have been linked to increased endothelial damage and impaired vascular function [31]. Furthermore, inflammation and increased perivascular infiltration of macrophages and T-lymphocytes has been linked to endothelial dysfunction leading to impaired vascular relaxation and hypertension via increased circulating levels of IL-6, TNFα, IL-1β, and IL-17 [32]. Elevations in the pro-inflammatory cytokine IL-6 have been demonstrated to decrease levels and activity of eNOS, which is crucial for endothelial dependent relaxation [33]. The vascular dysfunction following elevated inflammatory responses to AgNP may contribute to an altered coronary flow and the observed expansion of cardiac injury. The cardiovascular impact of the instillation of AgNP seems to wane over time, as alterations in vascular responses and to a lesser, non-statistically significant, degree expansion of cardiac I/R were both diminished from 1 to 7 days. Despite the diminished impact of AgNP on cardiac end-points, over time the profile of serum cytokines in response to IT instillation of AgNP did change from 1 to 7 days following exposure. Elevations in circulating cytokines may result from continued AgNP interactions with cells in the lung, stimulating cytokine release and providing an underlying systemic inflammatory condition [12].

Of interest, there appears to minimal inflammation in the lung in terms of gross histologic morphology, cell differentials and bronchoalveolar lavage protein, conforming the reports from other studies that do not report acute overt lung toxicity following exposure to AgNPs [10,23,34,35]. However, we report an increase in serum cytokine concentrations and cardiac injury following exposure to AgNP. This may suggest an inflammatory response to IT instillation of AgNP that does not remain localized to the lungs. The apparent interactions of AgNP with macrophages observed in this study and reported elsewhere [12,23,36–38] may promote cytokine release in the lungs resulting in a systemic inflammatory response through these cytokines. AgNP have been demonstrated to interact with mast cells and induce degranulation [8]. It is possible that a similar mechanism results in activation of macrophages and resulting cytokine release. Furthermore, interaction of AgNP with immune cells including macrophages via scavenger receptors may result in apoptosis and associated initiation of inflammatory cascades [37,39]. The persistent elevation of cytokines observed in AgNP exposed rats may be related to the bio-persistence of AgNP and continuing interaction with alveolar macrophages which has been observed in gold-core citrate capped AgNP [23].

The heart and lungs are interconnected in terms of anatomy and physiological function and suggest a potential for a close relationship between pulmonary toxicant exposure and cardiovascular compromise [40,41]. In this study, we have demonstrated pulmonary exposure to AgNP results in an expansion of cardiac I/R injury 1 day and 7 days following IT instillation. We suggest that exposure to AgNP results in elevations of several pro-inflammatory cytokines, which may act to prime the cardiovascular system to respond to the evocable ischemic insult with an exaggerated injury. While the assessment of cytokine concentrations of recovered BALF was not performed for this study; however the degree of inflammatory cytokine in the lungs has been investigated. Halberl and co-workers published results that found elevations in macrophage stimulating cytokines in BALF of AgNP 1 day following IT instillation of 70 nm AgNP [13]. At 1 day following IT instillation we have found a significant elevation in serum levels of several pro-inflammatory cytokines. In general in our model at 7 days post instillation, serum concentrations of most cytokines levels remained elevated. We also observed a small but significant expansion of cardiac I/R injury at 7 days versus 1 day, which may suggest that extent of cardiac injury cannot simply be accounted for solely by discreet measures of the serum cytokine profile or tied to the presence of a single cytokine.

Interestingly, serum cytokine concentrations increased in citrate exposed animals from 1 and 7 days post exposure, which may indicate a vehicle effect of pulmonary instillation of citrate that has not previously described. This increase in background cytokine concentrations may be associated with the slight, but non-statistically significant, increase in cardiac I/R injury in citrate-exposed animals from 1 to 7 days.

We investigated alterations in coronary artery responses following AgNP instillation to understand if the expansion of the ischemic damage in the cardiac tissue might be related to a change in the perfusion of the tissue post ischemia via this artery. Interestingly, we found that IT exposure to AgNP resulted in a depressed serotonin constrictor stress response. This finding contrasts other reports of IT exposure to various nanomaterials associated with

augmented vascular constrictor responses [18,42,43] and elevated mean arterial pressure [10]. We observed that IT instillation of citrate may also have vasoactive properties as stress generation to 5-HT was further reduced compared to coronary artery segment responses from naïve or AgNP instilled rats. This unexpected vehicle effect may mask a pro-constrictor effect of exposure to AgNP as the comparison between vehicle and AgNP coronary response shows a partially reversal of the attenuation of the citrate response. The observed suppression of the segments response to 5-HT suggest a possible influence of capping or vehicle on vascular reactivity. The role of the capping agents used to disperse nanomaterials has been subject of great interest and there is strong evidence that capping agent can impact a toxicity of the material on various cells types [38,44] raising the question would IT instillation of AgNP in a different vehicle result in a greater stress generation to 5-HT if not for the presence of a vehicle effect? We did observe a depressed maximal relaxation to the endothelial dependent relaxation agent acetylcholine corroborating the reports of impaired endothelial relaxation following other particle exposures [42,43]. In aggregate our results appear to reflect a poor vaso-reactivity of the coronary vascular segments but does not indicate an enhanced vaso-constrictive state of the coronary vasculature during reperfusion after ischemia that would contribute to the infract expansion. Measures of coronary perfusion itself would need to be conducted in other future studies to support that hypothesis.

The persistence of AgNP *in vivo* has been reported to exist for up to 56 days [23] our results appear to confirm a bio-persistence of silver in pulmonary associated tissues/cells for 7 days. This may result from slowed pulmonary clearance of particles administered by instillation compared to inhalation [45] or the dissolution and formulation of other NP or salt participates [24,36,46] The contribution of silver ions to the observed toxicity observed remains a possible mechanism. It has been reported that 20 nm citrate capped AgNP quickly dissolutes in water however, this dissolution can be slowed in the presence of dipalmitoylphosphatidylcholine a componenet of surfactant [23,47]. The combination of slowed Ag^+ ion dissolution paired with delayed lung clearance may contribute to the persistent toxicity observed in this study.

A secondary question can be raised regarding AgNP and potential cardiovascular toxicity: What, if any, contribution do silver ions have in the exacerbated myocardial I/R injury? In order to address that question, male SD rats were instilled with 200 μl of 1 mg/ml, 0.1 mg/ml, or 0.01 mg/ml concentrations of AgAc, a silver salt that dissociated to form Ag^+ in an aqueous solution. The concentrations selected represent a range of potential silver ion dissolution from the nanoparticles in the lungs ranging from 100% dissolution to 1%. Reports from the NIH Centers for Nanotechnology Health Implications Research Consortium meetings suggest that the dissolution rate from theses nanomaterials in *in vitro* settings can range from 1–30% dependent on the particle size and the initial suspension concentration [23]. Studies regarding the dissolution of silver ions from AgNP are difficult to conduct, however studies have evaluated the Ag dissolution rates of species of AgNP in culture media [36]. Our assessment of the cardiovascular impact of the IT of silver acetate at least for 1 day post exposure, was not equivalent in its impact on cytokine and vascular reactivity as that observed for AgNP exposure and may suggest other mechanisms for ionic

silver related CV toxicity than those associated with AgNP. Comparing I/R injury expansion from AgAc to AgNP we observe similar extent of injury at the highest concentration of AgAc as induced by AgNP. However, 1 mg/ml AgAc represents a complete *in vivo* dissolution and higher than expected based on *in vitro* studies. Instillation of 0.1 mg/ml AgAc also induced I/R injury equivalent to AgNP. These data allow us to suggest, based on comparisons of AgNP to AgAc concentration dependent I/R injury, if silver ion dissolution from the AgNP was responsible for the establishment of condition for the I/R injury it would be close to particle dissolution of greater than 10% within the first 24 hours. The lack of toxicity associated with the lowest concentration of silver acetate instillation is congruent with findings in other cell types whereby low concentrations of ionic silver were not associated with cytotoxicity, however high concentrations of silver may contribute to cytotoxicity [48,49]. The *in vitro* dissolution rate is dependent on concentration, so it may be the expansion of I/R injury at 24 hours post exposure is associated with processes effected by the rate of dissolution of Ag^+. It is likely that Ag^+ ions are at least partially responsible for the cardiovascular toxicity of AgNP due their concentration dependent ability to expand I/R injury 24 hours post IT instillation. The contribution ionic silver toxicity may be tempered by decreased silver dissolution rates from AgNP in the presence of pulmonary surfactant, as well as particle size dependent dissolution rates [50]. Exposure to 1 mg/ml AgAc also resulted in depressed coronary artery segment relaxation responses to ACh, which could explain the expansion of cardiac infarct expansion, however the mechanism why which silver ions directly contribute to impaired vascular reactivity in the absence of a strong inflammatory response remains unclear. The lower concentrations of AgAc, which likely correspond to real world dissolution rates did not result in a marked increase in infarct expansion suggesting that mechanisms of toxicity may differ between AgNP and AgAc.

Conclusion

Given the prevalence of AgNP in commercial applications, it is crucial to understand the potential impact of AgNP on cardiovascular function, inflammation and injury. Pulmonary exposure to AgNP is a likely exposure route for individuals involved in manufacturing processes involving both synthesis of AgNP or its incorporation into consumer goods. Additionally, consumers may be subject to pulmonary exposure to AgNP through products such as disinfecting sprays or deodorants. We have found that IT instillation of 20 nm AgNP results in a serum pro-inflammatory cytokine profile without apparent lung injury. The elevation in circulating cytokines can be associated with the expansion of cardiac ischemia/reperfusion injury observed at 1 day and 7 days post exposure and can be correlated with known cardiac injury. The potential role of circulating cytokine to enhance coronary vascular tone contributing to the ischemic injury may not be likely associated with anyone cytokine. Despite evidence that AgNP may elicit an inflammatory response that may contribute to cardiovascular toxicity, the mechanisms by which AgNP induces an inflammatory response or vascular dysfunction remain elusive. Herein we found cardiovascular toxicity resulting from a single exposure to AgNP out to 7 days post exposure. Further studies utilizing multiple AgNP exposures and smaller concentrations are required to determine the lower limit of adverse impact on the cardiovascular system. Additionally, although exposure to high concentrations of AgAc resulted in expansion of

cardiac I/R injury, exposure to AgAc did not result in the same elevations of circulating cytokines or changes in vascular reactivity associated with exposure to AgNP, suggesting that the toxicity of AgNP is not entirely associated with the dissolution of silver from the nanomaterials.

Supplementary Material

Refer to Web version on PubMed Central for supplementary material.

Acknowledgments

We would like to acknowledge Josh Volkan and Jillian Odom for their technical support with the vascular protocols, H+E staining and BALF cell differentials. This work was supported by resources of the National Institute of Environmental Health Sciences U19ES019525, U01ES020127, U19ES019544 and East Carolina University.

References

1. Oberdörster G, Oberdörster E, Oberdörster J. Nanotoxicology: an emerging discipline evolving from studies of ultrafine particles. Environ Health Perspect. 2005; 113:823–839. [PubMed: 16002369]
2. Mijnendonckx K, Leys N, Mahillon J, Silver S, Van Houdt R. Antimicrobial silver: uses, toxicity and potential for resistance. Biometals. 2013; 26:609–621. [PubMed: 23771576]
3. Rai M, Kon K, Ingle A, Duran N, Galdiero S, et al. Broad-spectrum bioactivities of silver nanoparticles: the emerging trends and future prospects. Appl Microbiol Biotechnol. 2014; 98:1951–1961. [PubMed: 24407450]
4. Kumar V, Jolivalt C, Pulpytel J, Jafari R, Arefi-Khonsari F. Development of silver nanoparticle loaded antibacterial polymer mesh using plasma polymerization process. J Biomed Mater Res A. 2013; 101:1121–1132. [PubMed: 23015534]
5. Silva RM, Anderson DS, Franzi LM, Peake JL, Edwards PC, et al. Pulmonary effects of silver nanoparticle size, coating, and dose over time upon intratracheal instillation. Toxicol Sci. 2015; 144:151–162. [PubMed: 25628415]
6. Wang X, Ji Z, Chang CH, Zhang H, Wang M, et al. Use of coated silver nanoparticles to understand the relationship of particle dissolution and bioavailability to cell and lung toxicological potential. Small. 2014; 10:385–398. [PubMed: 24039004]
7. Yang W, Shen C, Ji Q, An H, Wang J, et al. Food storage material silver nanoparticles interfere with DNA replication fidelity and bind with DNA. Nanotechnology. 2009; 20:085102. [PubMed: 19417438]
8. Aldossari AA, Shannahan JH, Podila R, Brown JM. Influence of physicochemical properties of silver nanoparticles on mast cell activation and degranulation. Toxicol In Vitro. 2015; 29:195–203. [PubMed: 25458489]
9. McShan D, Ray PC, Yu H. Molecular toxicity mechanism of nanosilver. J Food Drug Anal. 2014; 22:116–127. [PubMed: 24673909]
10. Roberts JR, McKinney W, Kan H, Krajnak K, Frazer DG, et al. Pulmonary and cardiovascular responses of rats to inhalation of silver nanoparticles. J Toxicol Environ Health A. 2013; 76:651–668. [PubMed: 23941635]
11. Quadros ME, Marr LC. Environmental and human health risks of aerosolized silver nanoparticles. J Air Waste Manag Assoc. 2010; 60:770–781. [PubMed: 20681424]
12. Park J, Lim DH, Lim HJ, Kwon T, Choi JS, et al. Size dependent macrophage responses and toxicological effects of Ag nanoparticles. Chem Commun (Camb). 2011; 47:4382–4384. [PubMed: 21390403]
13. Haberl N, Hirn S, Wenk A, Diendorf J, Epple M, et al. Cytotoxic and proinflammatory effects of PVP-coated silver nanoparticles after intratracheal instillation in rats. Beilstein J Nanotechnol. 2013; 4:933–940. [PubMed: 24455451]

14. Katwa P, Wang X, Urankar RN, Podila R, Hilderbrand SC, et al. A carbon nanotube toxicity paradigm driven by mast cells and the IL-(3)(3)/ST(2) axis. Small. 2012; 8:2904–2912. [PubMed: 22777948]
15. Urankar RN, Lust RM, Mann E, Katwa P, Wang X, et al. Expansion of cardiac ischemia/reperfusion injury after instillation of three forms of multi-walled carbon nanotubes. Particle and Fibre Toxicology. 2012; 9:38. [PubMed: 23072542]
16. Upadhyay S, Stoeger T, George L, Schladweiler MC, Kodavanti U, et al. Ultrafine carbon particle mediated cardiovascular impairment of aged spontaneously hypertensive rats. Part Fibre Toxicol. 2014; 11:36. [PubMed: 25442699]
17. Wold LE, Ying Z, Hutchinson KR, Velten M, Gorr MW, et al. Cardiovascular remodeling in response to long-term exposure to fine particulate matter air pollution. Circ Heart Fail. 2012; 5:452–461. [PubMed: 22661498]
18. Thompson LC, Urankar RN, Holland NA, Vidanapathirana AK, Pitzer JE, et al. C_{60} exposure augments cardiac ischemia/reperfusion injury and coronary artery contraction in Sprague Dawley rats. Toxicological Sciences. 2014; 138:365–378. [PubMed: 24431213]
19. Thompson LC, Frasier CR, Sloan RC, Mann EE, Harrison BS, et al. Pulmonary instillation of multi-walled carbon nanotubes promotes coronary vasoconstriction and exacerbates injury in isolated hearts. Nanotoxicology. 2014; 8:38–49. [PubMed: 23102262]
20. Danscher G, Stoltenberg M. Silver enhancement of quantum dots resulting from (1) metabolism of toxic metals in animals and humans, (2) in vivo, in vitro and immersion created zinc-sulphur/zinc-selenium nanocrystals, (3) metal ions liberated from metal implants and particles. Prog Histochem Cytochem. 2006; 41:57–139. [PubMed: 16949439]
21. Hacker GW, Grimelius L, Danscher G, Bernatzky G, Muss W, et al. Silver Acetate Autometallography-an Alternative Enhancement Technique for Immunogold-Silver Staining (Igss) and Silver Amplification of Gold, Silver, Mercury and Zinc in Tissues. J Histotech. 1988; 11:213–221.
22. Sheng L, Wang X, Sang X, Ze Y, Zhao X, et al. Cardiac oxidative damage in mice following exposure to nanoparticulate titanium dioxide. J Biomed Mater Res A. 2013; 101:3238–3246. [PubMed: 23553934]
23. Anderson DS, Patchin ES, Silva RM, Uyeminami DL, Sharmah A, et al. Influence of particle size on persistence and clearance of aerosolized silver nanoparticles in the rat lung. Toxicol Sci. 2015; 144:366–381. [PubMed: 25577195]
24. von Haehling S, Schefold JC, Lainscak M, Doehner W, Anker SD. Inflammatory biomarkers in heart failure revisited: much more than innocent bystanders. Heart Fail Clin. 2009; 5:549–560. [PubMed: 19631179]
25. Mehra VC, Ramgolam VS, Bender JR. Cytokines and cardiovascular disease. J Leukoc Biol. 2005; 78:805–818. [PubMed: 16006537]
26. Frangogiannis NG. Regulation of the inflammatory response in cardiac repair. Circ Res. 2012; 110:159–173. [PubMed: 22223212]
27. Toldo S, Mezzaroma E, Bressi E, Marchetti C, Carbone S, et al. Interleukin-1beta blockade improves left ventricular systolic/diastolic function and restores contractility reserve in severe ischemic cardiomyopathy in the mouse. J Cardiovasc Pharmacol. 2014; 64:1–6. [PubMed: 25006675]
28. Swirski FK, Nahrendorf M. Leukocyte behavior in atherosclerosis, myocardial infarction, and heart failure. Science. 2013; 339:161–166. [PubMed: 23307733]
29. Lin L, Knowlton AA. Innate immunity and cardiomyocytes in ischemic heart disease. Life Sci. 2014; 100:1–8. [PubMed: 24486305]
30. Kleinbongard P, Heusch G, Schulz R. TNFalpha in atherosclerosis, myocardial ischemia/reperfusion and heart failure. Pharmacol Ther. 2010; 127:295–314. [PubMed: 20621692]
31. Kim DW, Zloza A, Broucek J, Schenkel JM, Ruby C, et al. Interleukin-2 alters distribution of CD144 (VE-cadherin) in endothelial cells. J Transl Med. 2014; 12:113. [PubMed: 24885155]
32. Gomolak JR, Didion SP. A role for innate immunity in the development of hypertension. Med Hypotheses. 2014; 83:640–643. [PubMed: 25441337]

33. Cavieres V, Valdes K, Moreno B, Moore-Carrasco R, Gonzalez DR. Vascular hypercontractility and endothelial dysfunction before development of atherosclerosis in moderate dyslipidemia: role for nitric oxide and interleukin-6. Am J Cardiovasc Dis. 2014; 4:114–122. [PubMed: 25360389]
34. Kwon JT, Minai-Tehrani A, Hwang SK, Kim JE, Shin JY, et al. Acute pulmonary toxicity and body distribution of inhaled metallic silver nanoparticles. Toxicol Res. 2012; 28:25–31. [PubMed: 24278586]
35. Stebounova LV, Adamcakova-Dodd A, Kim JS, Park H, O'Shaughnessy PT, et al. Nanosilver induces minimal lung toxicity or inflammation in a subacute murine inhalation model. Part Fibre Toxicol. 2011; 8:5. [PubMed: 21266073]
36. Munusamy P, Wang C, Engelhard MH, Baer DR, Smith JN, et al. Comparison of 20 nm silver nanoparticles synthesized with and without a gold core: Structure, dissolution in cell culture media, and biological impact on macrophages. Biointerphases. 2015; 10:031003. [PubMed: 26178265]
37. Singh RP, Ramarao P. Cellular uptake, intracellular trafficking and cytotoxicity of silver nanoparticles. Toxicol Lett. 2012; 213:249–259. [PubMed: 22820426]
38. Shannahan JH, Podila R, Aldossari AA, Emerson H, Powell BA, et al. Formation of a Protein Corona on Silver Nanoparticles Mediates Cellular Toxicity via Scavenger Receptors. Toxicol Sci. 2015; 143:136–146. [PubMed: 25326241]
39. Eom HJ, Choi J. p38 MAPK activation, DNA damage, cell cycle arrest and apoptosis as mechanisms of toxicity of silver nanoparticles in Jurkat T cells. Environ Sci Technol. 2010; 44:8337–8342. [PubMed: 20932003]
40. Bhaskaran K, Hajat S, Haines A, Herrett E, Wilkinson P, et al. Effects of air pollution on the incidence of myocardial infarction. Heart. 2009; 95:1746–1759. [PubMed: 19635723]
41. Uzoigwe JC, Prum T, Bresnahan E, Garelnabi M. The emerging role of outdoor and indoor air pollution in cardiovascular disease. N Am J Med Sci. 2013; 5:445–453. [PubMed: 24083218]
42. Vidanapathirana AK, Thompson LC, Odom J, Holland NA, Sumner SJ, et al. Vascular Tissue Contractility Changes Following Late Gestational Exposure to Multi-Walled Carbon Nanotubes or their Dispersing Vehicle in Sprague Dawley Rats. Journal of Nanomedicine & Nanotechnology. 2014; 5
43. Vidanapathirana AK, Thompson LC, Mann EE, Odom JT, Holland NA, et al. PVP formulated fullerene (C60) increases Rho-kinase dependent vascular tissue contractility in pregnant Sprague Dawley rats. Reprod Toxicol. 2014; 49C:86–100. [PubMed: 25088243]
44. Wang X, Xia T, Duch MC, Ji Z, Zhang H, et al. Pluronic F108 coating decreases the lung fibrosis potential of multiwall carbon nanotubes by reducing lysosomal injury. Nano Lett. 2012; 12:3050–3061. [PubMed: 22546002]
45. Pritchard JN, Holmes A, Evans JC, Evans N, Evans RJ, et al. The distribution of dust in the rat lung following administration by inhalation and by single intratracheal instillation. Environ Res. 1985; 36:268–297. [PubMed: 3979359]
46. Smulders S, Larue C, Sarret G, Castillo-Michel H, Vanoirbeek J, et al. Lung distribution, quantification, co-localization and speciation of silver nanoparticles after lung exposure in mice. Toxicol Lett. 2015; 238:1–6. [PubMed: 26162856]
47. Seiffert J, Hussain F, Wiegman C, Li F, Bey L, et al. Pulmonary toxicity of instilled silver nanoparticles: influence of size, coating and rat strain. PloS One. 2015; 10:e0119726. [PubMed: 25747867]
48. Stoehr LC, Gonzalez E, Stampfl A, Casals E, Duschl A, et al. Shape matters: effects of silver nanospheres and wires on human alveolar epithelial cells. Part Fibre Toxicol. 2011; 8:36. [PubMed: 22208550]
49. Foldbjerg R, Irving ES, Hayashi Y, Sutherland DS, Thorsen K, et al. Global gene expression profiling of human lung epithelial cells after exposure to nanosilver. Toxicol Sci. 2012; 130:145–157. [PubMed: 22831968]
50. Leo BF, Chen S, Kyo Y, Herpoldt KL, Terrill NJ, et al. The stability of silver nanoparticles in a model of pulmonary surfactant. Environ Sci Technol. 2013; 47:11232–11240. [PubMed: 23988335]

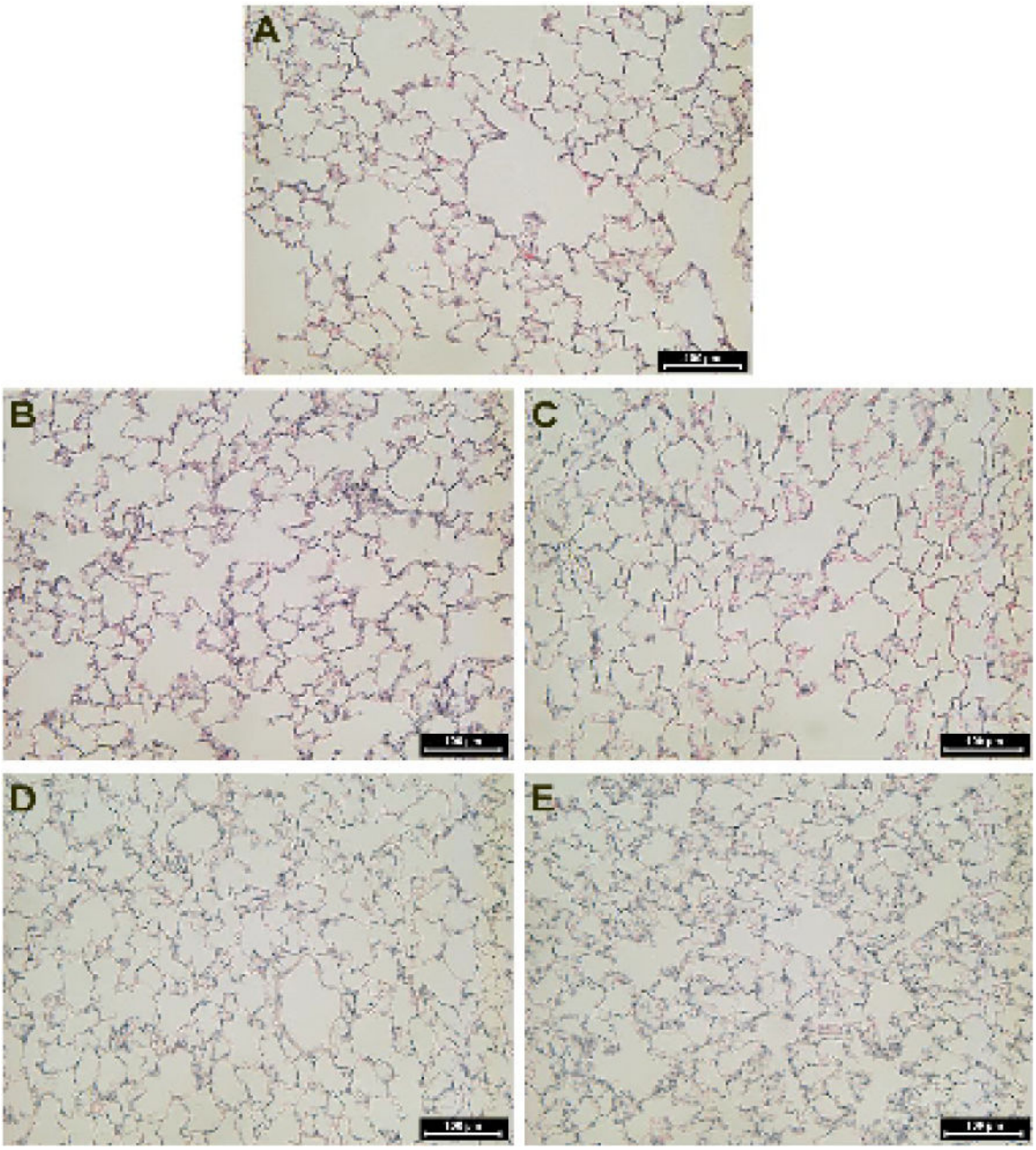

Figure 1.

H&E lung histology. Representative images of hematoxylin and eosin stained lung histology sections. Naïve Sprague Dawley Rat (A), 1 day following citrate vehicle instillation (B), 7 days following instillation of citrate vehicle (C), 1 day following instillation of 20 nm AgNP (D), 7 days following instillation of 20 nm AgNP (E). No gross pathology was noted in the naïve cohort or within the citrate vehicle or 20 nm AgNP at 1 day. The citrate vehicle had some erythrocytes within the lung tissue while the 20 nm AgNP showed modset increased alveolar wall thickening at 7 days post instillation. Back bar identifies 50 μm scaling.

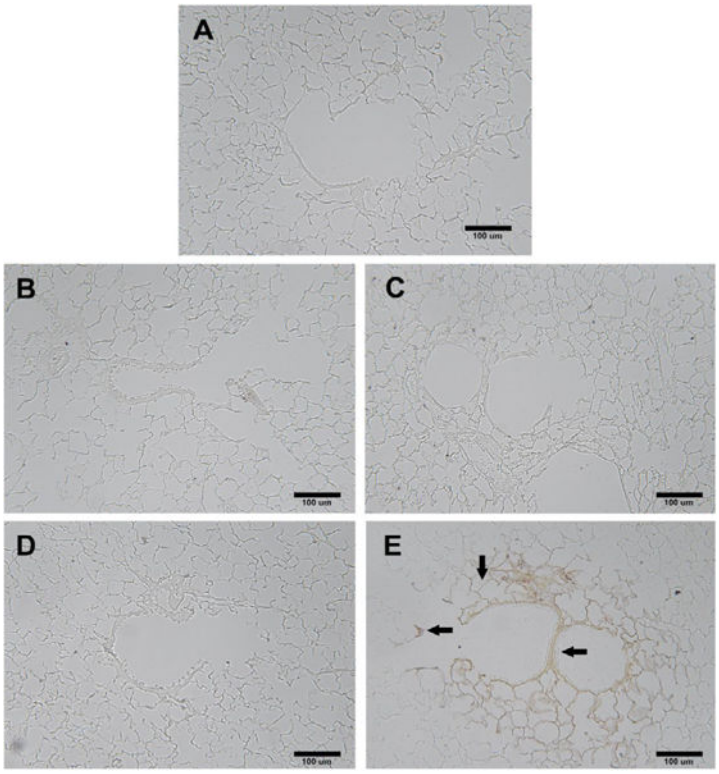

Figure 2.

Autometalography silver staining of lungs. Silver localization in lung tissue at the terminal bronchiole alveolar duct junction using autometallography with no background staining. Arrows show localization of silver to the terminal bronchiole alveolar duct junction 7 days post instillation. Silver is particularly associated with bifurcations, and the subepithelial extracellular matrix and adjacent vasculature. Panel A) Naïve; B) Citrate vehicle 1 day; C) Citrate vehicle 7 days; D) AgNP 1 day and E) AgNP 7 days post instillation. Back bar identifies100 μm scaling.

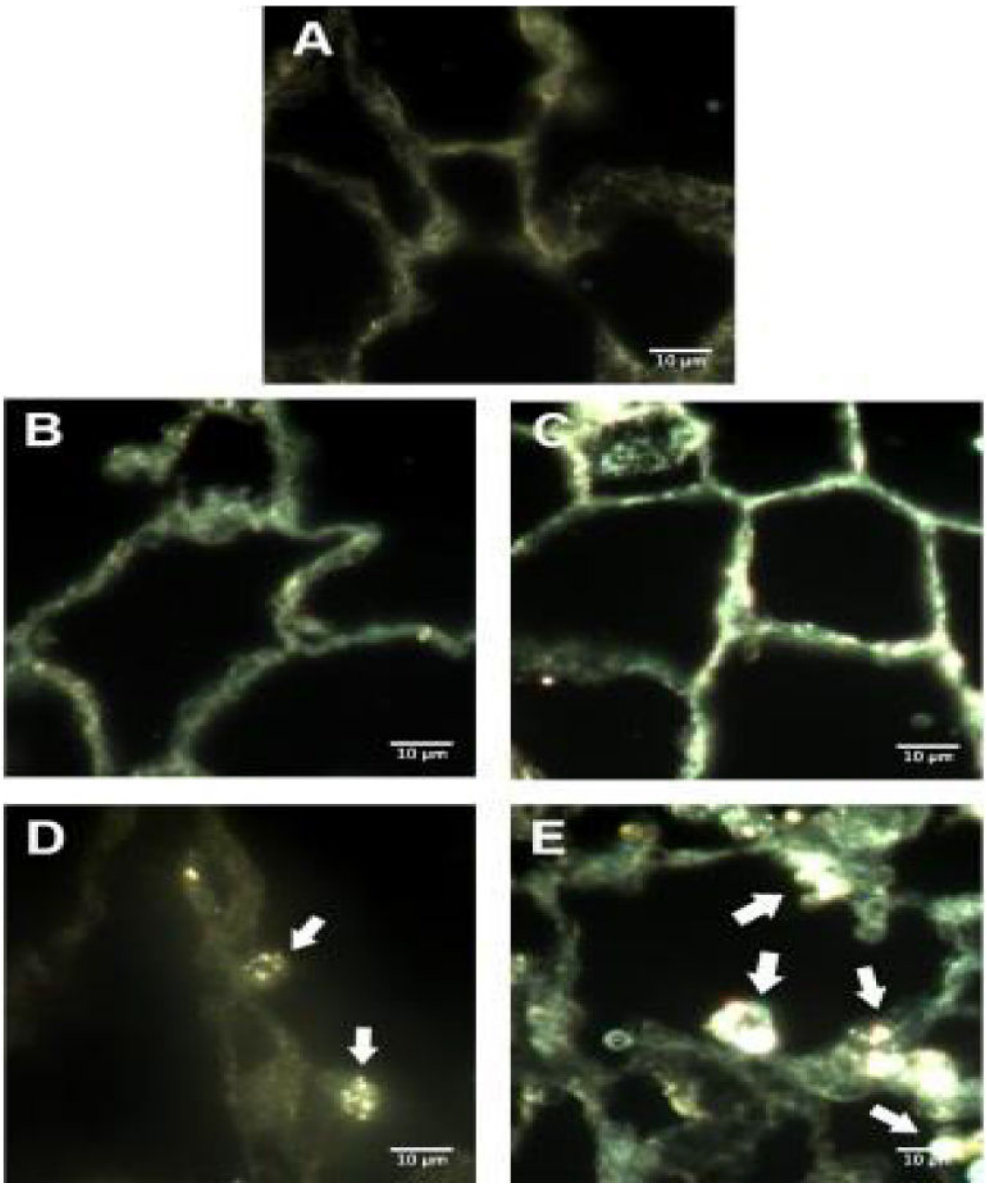

Figure 3.

Darkfield microscopy of lung histology. Representive images of enchanced darkfield microsopy of lung tissue. Naïve male Sprague-Dawley Rat (A), 1 day following citrate vehicle instillation (B), 7 days following instillation of citrate vehicle (C), 1 day following instillation of 20 nm AgNP (D), 7 days following instillation of 20 nm AgNP (E). White arrows indicate punctate formations of AgNP visible in sections. White bar identifies 10 μm scaling.

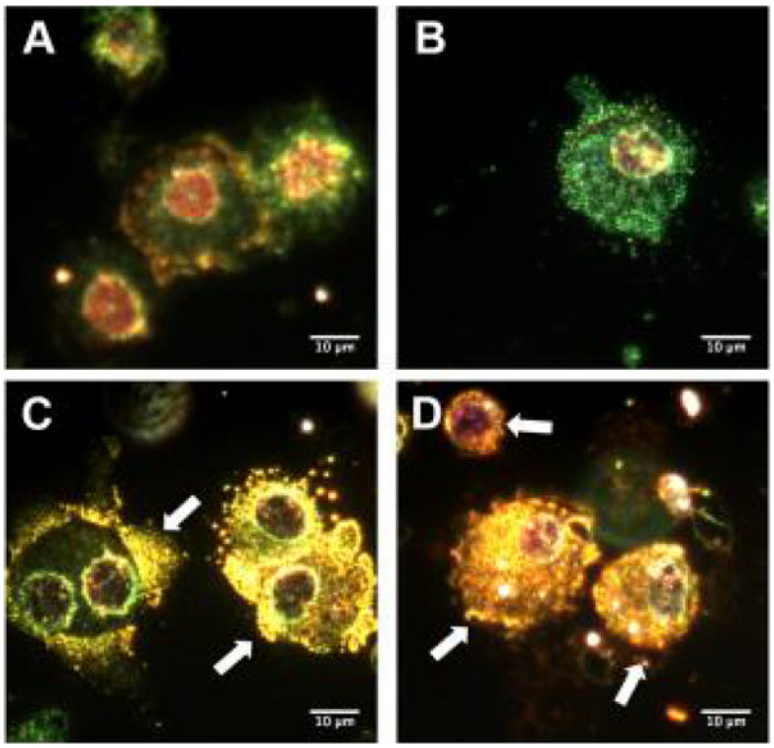

Figure 4.

Darkfield microscopy of isolated BAL cells. Representive images of enchanced darkfield microsopy of cells recovered from bronchoalveolar lavage fluid. One day following citrate vehicle instillation (A), 7 days following instillation of citrate vehicle (B), 1 day following instillation of 20 nm AgNP (C), 7 days following instillation of 20 nm AgNP (D). White bar identifies 10 μm scaling. White arrows indicate the punctate accumulation of silver particles associated with alveolar macrophages.

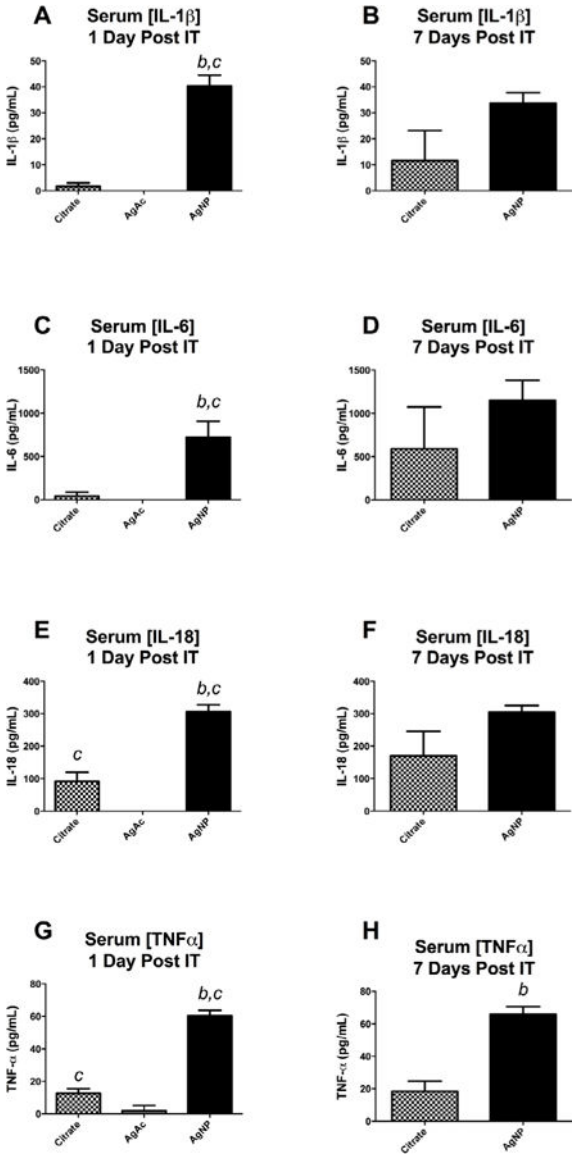

Figure 5.

Serum proinflammatory cytokine concentrations following IT instillation of AgNP or AgAc. Serum concentration of proinflammatory cytokines 1 day and 7 days after IT instillation. Cytokines IL-1β (A), IL-6 (C), IL-18 (D), and TNFα (E) were elevated compared to citrate vehicle 1 day following IT instillation. At 7 days following instillation only TNFα (H) remained elevated above vehicle. *b* denotes statistical significance from vehicle. *c* denotes difference compared to 1mg/ml AgAc $p<0.05$ by t-test, Data are reported as mean ± SEM with n=4–5.

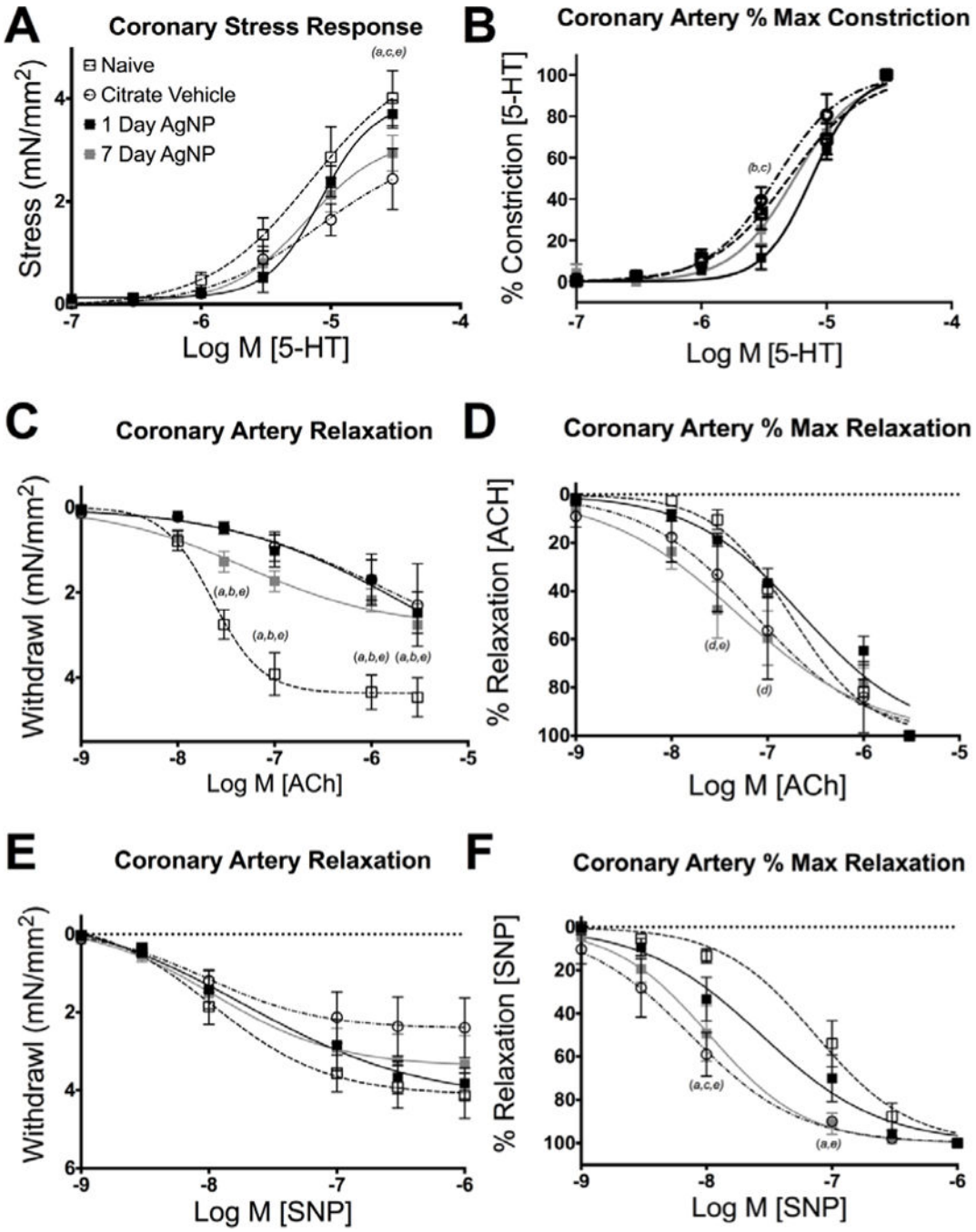

Figure 6.

Coronary artery myography responses. Pharmacologic responses of coronary artery segments including: maximal stress response to 5-HT (A), and percent maximal constrictor response to 5-HT (B), maximal stress relaxation to ACh (C) and SNP (E), Percent relaxation of maximal stress to ACh (D) and SNP (F). Significance expressed as $p<0.05$ as follows: (*a*) Naïve vs Citrate vehicle, (*b*) Naïve vs. 1 day, (*c*) Citrate vehicle vs 1 day AgNP, (*d*) 1 day vs 7 day AgNP, (*e*) Naïve vs 7 day AgNP. Data are reported as mean ± SEM with n=4–6, Lines represent the nonliner Hill fit to the mean values.

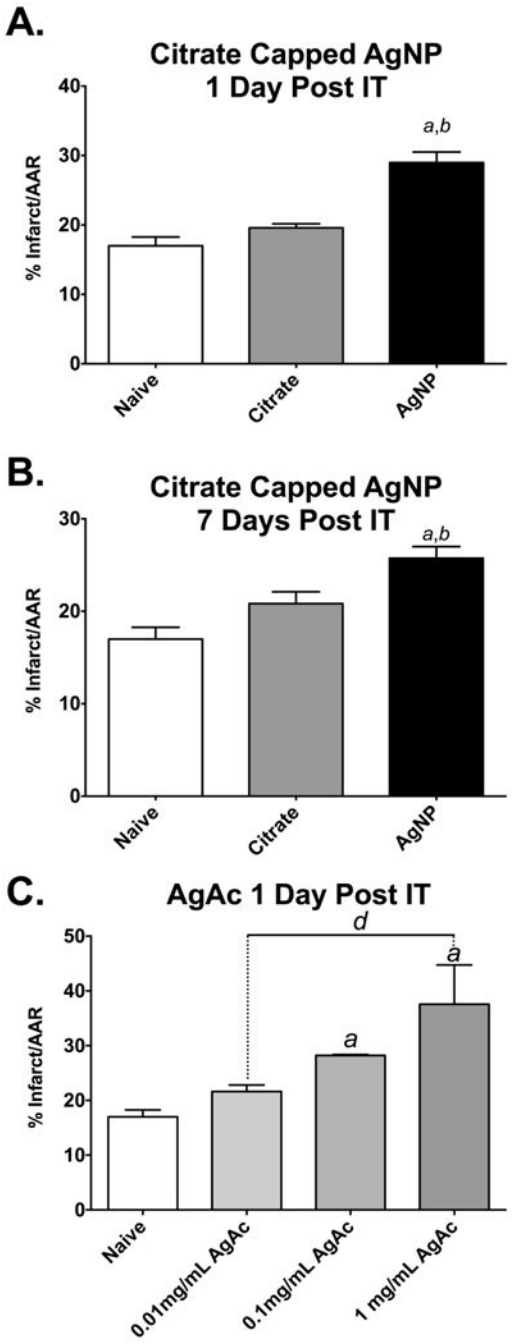

Figure 7.

Cardiac ischemia/reperfusion injury following IT instillation of AgNP and AgAc. Cardiac I/R injury in male SD rats exposed to 200 μl of citrate vehicle or 200 μg AgNP or 2–200 μg silver acetate (AgAc) following 20 minutes of ischemia and 2 hours of reperfusion. Ischemia-reperfusion injury is expanded 1 day following IT exposure to AgNP compared to vehicle or naïve (A). Expansion of I/R injury persists 7 days following IT instillation (B). Male SD rats exposed to IT instillation of 0.01 mg/mL (2 μg), 0.1 mg/mL(20 μg), or 1 mg/mL(200 μg) AgAc. I/R injury is expanded 24 hours following IT exposure to the two highest

concentrations of AgAc (C). *a* significant versus naïve, *b* significant vs vehicle, *d* vs 1mg/mL AgAc. Data are reported as mean ± SEM with n=3–4.

Table 1

Bronchoalveolar lavage cell differentials: Total cell number and relative percentage of macrophages, neutrophils, eosinophils, lyphocytes, and epithelial cells present in BAL fluid following 200 μl IT instillation of citrate vehicle, 200 μg 20 nm AgNP or silver acetate (AgAc). Statistical significance was determined as $p<0.05$ compared to naïve a or citrate vehicle b by one way ANOVA with Tukey post hoc test. n=4–5. Data reported as mean ± SEM.

	TotalCells ($\times 10^5$)	Macrophages (% of Total cell count)	Neutrophils (% of Total cell count)	Eosinophils (% of Total cell count)	Lympocytes (% of Total cell count)	Epitheila Cells (% of Total cell count)
Naive	3.2 ± 0.6	99.1 ± 0.2	0.1 ± 0.1	0.0 ± 0.0	0.0 ± 0.0	0.8 ± 0.2
Citrate Vehicle	2.7 ± 0.5	95.9± 0.7	0.1 ± 0.1	0.1 ± 0.1	0.2 ± 0.1	3.8 ± 0.7[a]
AgNP (1day)	4.1 ± 0.6	90.8 ± 7.7	7.8 ± 7.7	0.0 ± 0.0	0.7 ± 0.7	0.7 ± 0.4[b]
AgNP (7day)	3.7 ± 0.7	89.1 ± 5.1	8.9 ± 5.1	0.4 ± 0.2	0.8 ± 0.3	0.8 ± 0.4[b]
AgAc (1day)	6.1 ± 1.1[a,b,c]	57.6 ± 10.8	37.8 ± 10.2[a,b,c]	0.2 ± 0.2	3.9 ± 1.1	0.5 ± 0.4

Note: Total cells and reletive percentage of macrophages, neutrophils, eosinophils, lyphocytes, and epithelial cells present in BAL fluid following IT instillation of citrate vehicle or 200 μg in 200 μl installation blous of 20 nm silver naoparticle (AgNP) or silver acetate (AgAc). Statistical significance $p<0.05$ compared to

[a] naïve,

[b] Citrate vehicle,

[c] 1 day AgNP, determined by one way ANOVA with Tukey post hoc test. Data displayed as mean ± SEM, n=4–5.

Table 2

Bronchoalveolar Lavage Protein Quantification: Protein concentration measured by Bradford assay from recovered BAL Fluid following 200 µl IT instillation of citrate vehicle, 200 µg 20 nm AgNP or silver acetate (AgAc). Statistical significance $p<0.05$ compared to ^{a}naïve or ^{b}citrate vehicle determined by one way ANOVA with Tukey post hoc test. n=4–5. Data reported as mean ± SEM.

	Total Protein (mg/ml)
Naive	0.15 ± 0.01
Citrate Vehicle	
1 d	0.31 ± 0.09
7 d	0.22 ± 0.02
AgNP	
1 d	0.33 ± 0.02
7 d	0.18 ± 0.03
AgAc	3.88 ± 2.25

Note: Protein concentration measured by Bradford assay from recovered BAL fluid. Silver nanoparticle (AgNP) or silver acetate (AgAc) was deliverd as a 200 µg in 200 µl installation blous. Statistical significance $p<0.05$ compared to naïve or Citrate vehicle determined by one way ANOVA with Tukey post hoc test. n=4–5. Data displayed as mean ± SEM.

Table 3

Serum cytokines and chemokines: Serum cytokine concentrations 1 and 7 days following instillation 200 μl of citrate vehicle 200 μg 20 nm AgNP or 1 day post silver acetate (AgAc) instillation. Statistical significance $p<0.05$ compared to citrate vehicle b determined by student's t-test. n=4–5. Data reported as mean ± SEM.

Cytokine/Chemokine (pg/ml)	Citrate		AgNP		AgAc
	1 day	7 days	1 day	7 days	1 day
G-CSF	11.1 ± 3.93	53.0 ± 38.1	90.6 ± 21.1[b,c]	119.0±14.5	0.0 ± 0.0
GM-CSF	0.0 ± 0.0	10.9 ± 10.9	0.0 ± 0.0	0.0 ± 0.0	0.0 ± 0.0
MIP-1α	20.9 ± 3.7[c]	28.2 ± 8.9	41.5 ± 1.53[b,c]	40.4 ± 1.49	0.0 ± 0.0
IL-2	110.0 ± 29.3[c]	175.0 ± 65.3	312.0 ± 10.1[b,c]	328 ± 23.3[b]	0.0 ± 0.0
IL-13	0.0 ± 0.0	20.7 ± 20.7	422.0 ± 155.0[b,c]	792 ± 224[b]	0.0 ± 0.0
IL-10	23.9 ± 8.1[c]	51.3 ± 31.2	101.0 ± 5.4[b,c]	99.8 ± 9.51	0.0 ± 0.0
INFγ	0.0 ± 0.0	187.0±187.0	126.0 ± 126.0	305.0 ± 39.6	0.0 ± 0.0
IL-5	243 ± 43.6	351.0 ± 79.6	331.0 ± 7.8	324.0 ± 7.82	8.74 ± 8.74
IL-17α	54.6 ± 18.3[c]	94.7 ± 37.9	155.0 ± 7.8[b,c]	167 ± 8.32	0.0 ± 0.0
RANTES	721.0 ± 26.8[c]	663.0 ± 130.0	1138.0 ± 52.1[b,c]	924.0 ± 60.4	143 ± 13.7

Note: Serum cytokine concentrations 1 day and 7 days following 200μl instillation of Citrate vehicle or 200 μg 20 nm AgNP or silver acetate (AgAc). Statistical significance $p<0.05$ compared to

[b] Citrate vehicle at matched time-point or compaired to

[c] AgAc determined by one-way ANOVA and Tukey's post-hoc test for multiple compairisions. Data displayed as mean ± SEM, n=4–5.

Table 4

Pharmacology of the Isolated Coronary Artery Segments: Calculated EC50, Hillslope, Minimum Stress, and Maximum stress responses of LAD coronary artery segment to serotonin (5-HT), acetylcholine (ACh), and sodium nitroprusside (SNP) 1 day and 7 days following 200 μl instillation of Citrate vehicle or 200 μg 20 nm AgNP or 1 day post silver acetate (AgAc) instillation. Values expressed ± SEM. (a) denotes significant versus Naïve ($p<0.05$), (b) denotes significant versus citrate vehicle ($p<0.05$).

		EC_{50} (nM)	Hillslope	Maximum Stress Withdrawl (mN/mm^2)	Maximum Stress Constriction (mN/mm^2)
5-HT	**Naïve**	5623 ± 1304	1.67 ± 0.18		4.01 ± 0.53
	Citrate	4805 ± 859	1.91 ± 0.20		2.44 ± 0.59
	AgNP				
	1d	7769 ± 908	3.49 ± 0.50[ab]		3.70 ± 0.27
	7d	6142 ± 980	2.65 ± 0.38		2.94 ± 0.35
	AgAc	4472 ± 819	1.75 ±0.12		2.38 ± 0.52
ACh	**Naïve**	184 ± 39	1.17 ± 0.13	4.46 ± 0.46	
	Citrate	190 ± 149	1.06 ± 0.20	2.30 ± 0.97	
	AgNP				
	1d	261 ± 65	0.82 ± 0.07	2.47 ± 0.49	
	7d	94 ± 31	1.00 ± 0.34	2.76 ± 0.49	
	AgAc	136 ± 199	1.08 ± 0.06	1.56 ± 0.45[a]	
SNP	**Naïve**	98 ± 29	1.94 ± 0.32	4.14 ± 0.58	
	Citrate	9 ± 3[a]	1.28 ± 0.09	2.40 ± 0.76	
	AgNP				
	1 d	51 ± 23	1.68 ± 0.32	3.83 ± 0.39	
	7d	14 ± 4[a]	1.49 ± 0.19	3.33 ± 0.73	
	AgAc	60 ± 15	1.64 ± 0.14	2.85 ± 0.86	

Calculated EC_{50}, Hillslope, Minimum Stress, and Maximum stress responses of LAD coronary artery segment to serotonin (5-HT), acetylcholine (ACh), and sodium nitroprusside (SNP) 1 day and 7 days following 200 μl instillation of Citrate vehicle or 200 μg 20 nm AgNP or 1 day post silver acetate (AgAc) instillation. Values reported as Mean ± SEM. Statistical significance $p<0.05$ compared to

[a] naïve,

[b] Citrate vehicle, 1 day AgNP determined by one way ANOVA with Tukey post hoc test. Data displayed as mean ± SEM, n=4–6.